

# Construction of Left Ventricle 3D Shape Atlas from Cardiac MRI

Shaoting Zhang<sup>1</sup>, Mustafa Uzunbas<sup>1</sup>, Zhennan Yan<sup>1</sup>, Mingchen Gao<sup>1</sup>,  
Junzhou Huang<sup>1</sup>, Dimitris N. Metaxas<sup>1</sup> and Leon Axel<sup>2</sup>

<sup>1</sup>Rutgers, the State University of New Jersey, Computer Science Department

<sup>2</sup>New York University, Radiology Department

**Abstract.** In this paper, we present an effective algorithm to construct a 3D shape atlas for the left ventricle of heart from cardiac Magnetic Resonance Image data. We derive a framework that creates a 3D object mesh from a 2D stack of contours, based on geometry processing algorithms and a semi-constrained deformation method. The geometry processing methods include decimation, detail preserved smoothing and isotropic remeshing, and they ensure high-quality meshes. The deformation method generates subject-specific 3D models, but with global point correspondences. Once we extract 3D meshes from the sample data, generalized Procrustes analysis and Principal Component Analysis are then applied to align them together and model the shape variations. We demonstrate the algorithm via a set of experiments on a population of cardiac MRI scans. We also present modes of variation from the computed atlas for the control population, to show the shape and motion variability.

## 1 Introduction

In the last decade, Magnetic Resonance Imaging (MRI) has been proven to be a non-invasive tool that can be used to measure the myocardial mass and functional deformation of the heart [8]. Quantification of ventricular mass and function are important for early diagnosis of cardiac disorders and quantitative analysis of cardiac diseases. Recent developments in Cine MRI further help diagnose the presence of heart disease by analyzing the heart function throughout the cardiac cycle. MRI is becoming considered as a gold-standard for cardiac function [2, 6]. In this context, the construction of an anatomical shape atlas of the structures in the heart has been of particular interest and its importance has been emphasized in a number of recent studies [10, 11, 13].

In clinical applications, particularly the delineation of left ventricle endocardium and epicardium, automatic and quantitative approaches are highly desired to facilitate the analysis of comprehensive MR data sets. Regarding the needs for automated and quantitative methods in clinical applications, an atlas can provide a reference shape for a family of shapes or can be used to model the consistent deformation of a structure of interest. This could be useful in numerous applications including, but not limited to, statistical analysis of different populations, the segmentation of structures of interest, motion characterization, functional analysis, and the detection of various diseases [5, 11, 13]. The 3D size and shape characteristics of the left ventricle, and its deformation over a cardiac cycle, are relatively consistent and can be fairly well characterized by specific

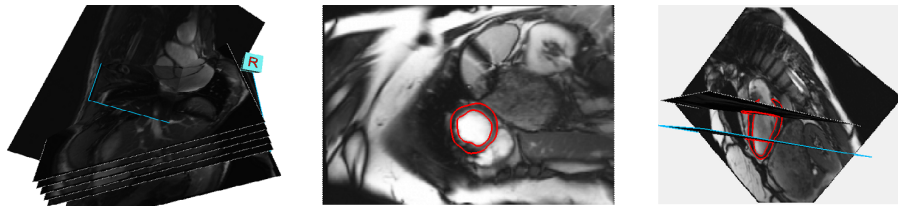


**Fig. 1.** From left to right: visualization of 2D slices from MR scans; annotation in the short axis; annotation in the long axis.

models. 2D delineations of the left ventricle is already available from manual segmentation. Accurate 3D manual annotation, however, is difficult and time-consuming.

In this paper, we propose a method for creating a 3D shape atlas of the left ventricle from 2D manual delineations. It employs currently available 2D databases and could lead to further novel segmentation methods if further developed. The input to our algorithm is a cloud of points marked on a set of sparse, 2D cardiac slices, as shown in Fig. 1. Note here, that the slice thickness is typically several times larger than the pixel size in cardiac MR images, so that the resolution is poorer in the direction orthogonal to the slice. Thus, creating a 3D model from such sparse data is challenging. Our proposed framework is based on several steps. First, a 3D binary image is generated by interpolating 2D labeling. Then a surface is obtained from the 3D binary file, using Marching Cubes algorithm. Second, geometry processing methods are applied to obtain a high quality mesh. These methods include decimation, detail-preserved smoothing, and isotropic remeshing. In the third step, the one-to-one correspondence for each vertex is obtained among the sample set of the model by registering a reference shape model to all the other samples. The transformation is done based on a nonrigid local deformation method. The mapping of a unique template to all instances provides a consistency among not only the motion model of one cardiac image series, but also shape and textures model of many cardiac series from different patients, if needed. In the final step, shape statistics are computed straightforwardly, using generalized Procrustes analysis and PCA. The mean shape and major variations are then obtained. Note here, that the manual delineations do not have to be constrained with any anatomical point correspondence. Our method automatically resolves that issue, both among multiple instances of the same phase of a cardiac cycle or sequential phases of one cycle. The ability to fit the atlas to all temporal phases of a dynamic study can benefit the automatic functional analysis.

## 2 Methods

### 2.1 Algorithm Framework

Fig. 2 shows the algorithm framework. The typical input data is MRI scans, acquired in different locations, along with their 2D contour labeling. The MRI data can be relatively sparse. Note that the input data can also be previously constructed 3D binary images or meshes. In such cases the algorithm will just start from the second or the

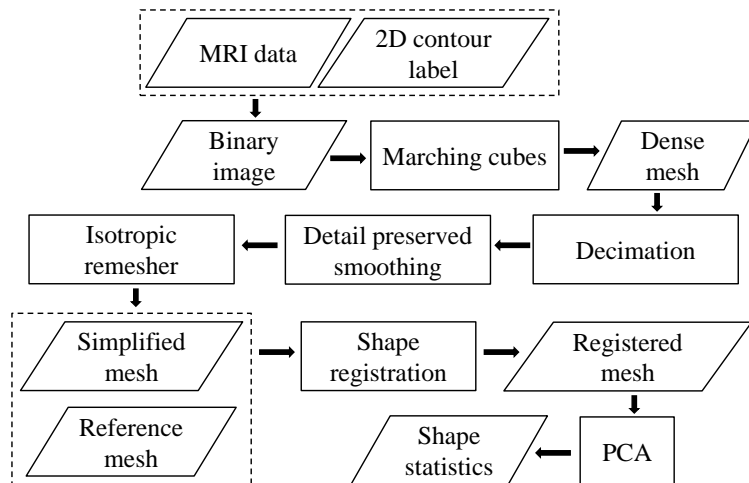


**Fig. 2.** The algorithm flowchart. The diamond shape represents data, and the rectangular shape denotes algorithms.

third step. Given MRI and 2D contour data, a 3D binary image is generated by interpolating values among slices. Then, the Marching Cubes method [4] is employed to derive the corresponding isosurfaces. The mesh of this surface may be very dense and contain hundreds of thousands vertices. Furthermore, the shape of this may contain artifacts caused by the sharp transitions at contours. It is necessary to downsample and smooth it, without removing the shape detail information. After these geometry processing steps, a simplified and high-quality shape is generated. Then, a reference shape is deformed to fit it, using a shape registration method. Since all resulting shapes are registered with the same reference shape, they share the same topology and all vertices have one-to-one correspondences. Finally, generalized Procrustes analysis [1, 3] and Principal Component Analysis (PCA) are used to compute the mean shape and major variations.

## 2.2 Geometry Processing

In our system, the input data is converted to a isosurface after the preprocessing. Because of the properties of Marching Cubes, such surface may contain too many vertices and also may have local artifacts. Thus it is desirable to obtain a simplified and high-quality mesh, with shape details preserved. We use mesh decimation to downsample the input shape, and also use isotropic remeshing to guarantee that each vertex has six neighbors. The remaining difficulty is to smooth the shape without losing the important details. We use Laplacian Surface Optimization [7] to achieve this. This method has previously been employed to reconstruct the left ventricle from tagged MRI [12].

Let the mesh  $\mathbb{M}$  of the shape be described by a pair  $(\mathbb{V}, \mathbb{E})$ , where  $\mathbb{V} = \{v_1, \dots, v_n\}$  describes the geometric positions of the vertices in  $\mathbb{R}^3$  and  $\mathbb{E}$  describes the connectivity. The neighborhood ring of a vertex  $i$  is the set of adjacent vertices  $\mathbb{N}_i = \{j | (i, j) \in$

$\mathbb{E}$ } and the degree  $d_i$  of this vertex is the number of elements in  $\mathbb{N}_i$ . Instead of using absolute coordinates  $\mathbb{V}$ , the mesh geometry is described as a set of differentials  $\Delta = \{\delta_i\}$ . Specifically, coordinate  $i$  will be represented by the difference between  $v_i$  and the weighted average of its neighbors:  $\delta_i = v_i - \sum_{j \in \mathbb{N}_i} w_{ij} v_j$ , where  $w_{ij}$  is computed from cotangent weights [7]. Assume  $V$  is the matrix representation of  $\mathbb{V}$ . Using a small subset  $\mathbb{A} \subset \mathbb{V}$  of  $m$  anchor points, a mesh can be reconstructed from connectivity information alone. The  $x$ ,  $y$  and  $z$  positions of the reconstructed object ( $V'_p = [v'_{1p}, \dots, v'_{np}]^T, p \in \{x, y, z\}$ ) can be solved for separately by minimizing the quadratic energy:

$$\|L_u V'_p - \Delta\|^2 + \sum_{a \in \mathbb{A}} \|v'_{ap} - v_{ap}\|^2, \quad (1)$$

where  $L_u$  is the Laplacian matrix from uniform weights, and the  $v_{ap}$  are anchor points.  $\|L_u V'_p - \Delta\|^2$  tries to smooth the mesh when keeping it similar to the original shape, and  $\sum_{a \in \mathbb{A}} \|v'_{ap} - v_{ap}\|^2$  keeps the anchor points unchanged. The cotangent weights approximate the normal direction, and the uniform weights point to the centroid. By minimizing the difference of these two (i.e.,  $L_u V'$  and  $\Delta$ ), the vertex is actually moved along the tangential direction. Thus the shape is smoothed without significantly losing the detail. With  $m$  anchors, (1) can be rewritten as a  $(n + m) \times n$  overdetermined linear system  $AV'_p = b$ :

$$\begin{bmatrix} L_u \\ I_{ap} \end{bmatrix} V'_p = \begin{bmatrix} \Delta \\ V_{ap} \end{bmatrix} \quad (2)$$

This is solved in the least squares sense using the method of normal equations  $V'_p = (A^T A)^{-1} A^T b$ . The conjugate gradient method is used in our system to efficiently solve it. The first  $n$  rows of  $AV'_p = b$  are the Laplacian constraints, corresponding to  $\|L_u V'_p - \Delta\|^2$ , while the last  $m$  rows are the positional constraints, corresponding to  $\sum_{a \in \mathbb{A}} \|v'_{ap} - v_{ap}\|^2$ .  $I_{ap}$  is the index matrix of  $V_{ap}$ , which maps each  $V'_{ap}$  to  $V_{ap}$ . The reconstructed shape is generally smooth, with the possible exception of small areas around anchor vertices.

### 2.3 Shape Registration and Shape Statistics

These simplified and high-quality meshes do not share the same topology. They may have different numbers of vertices, and there is no one-to-one correspondence for each vertex. Our solution is to use shape registration to deform a reference shape to fit to all the others. Since all deformed shapes are registered to the reference one, they effectively have one-to-one correspondences for each vertex. It is also important that the deformed reference shape should be almost identical to the target shape. We use an Adaptive-Focus Deformable Model (AFDM) [9] to do the shape registration task. This algorithm was originally designed for automatic segmentation and has the property of maintaining the topology. We have simplified it for shape registration without using image information. After applying AFDM for each shape, all shapes share the same topology.

Once the one-to-one correspondence is obtained for each vertex among all shapes, the shape statistics can be computed straightforwardly using generalized Procrustes

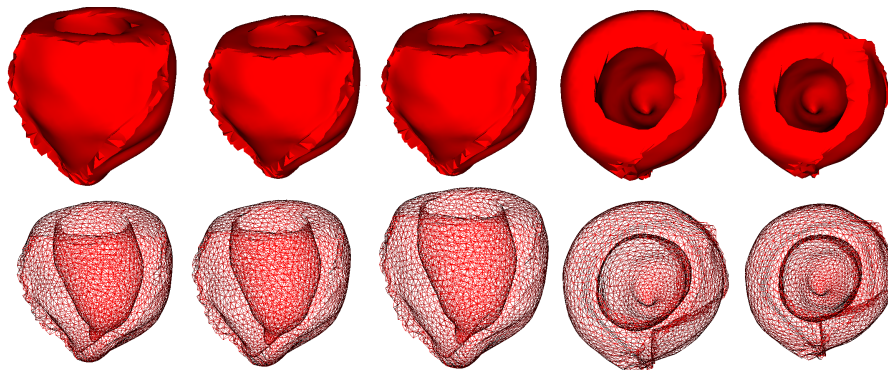


**Fig. 3.** Samples of decimated 3D meshes. The artifacts along the long axis can still be observed. Note that these shapes don't have one-to-one correspondence for vertices.

analysis and PCA, like the Active Shape Model [1] does. Given any two shapes, they can be fitted to each other using a similarity transformation. Procrustes analysis is used to find the translational, rotational and scaling components. Since there is no mean shape in the beginning, generalized Procrustes analysis arbitrarily chooses a shape to use as the reference and transforms all the rest to fit it. After that, a mean shape is computed by averaging all transformed shapes. Then, this mean shape is used as a reference shape in the next round. We repeat this procedure until the mean shape converges to a stable state. Note that normalization is necessary, as otherwise the mean shape will degenerate to a single point.

After the alignment, each resulting shape is filled into a matrix as a column vector. PCA is applied to get the Point Distribution Model (PDM). The important “modes” (i.e., eigenvectors corresponding to the largest eigenvalues) are selected to cover more than 80% of the variance. Combining the mean shape and the modes, the PDM is able to summarize and describe the sample shapes concisely and accurately. Such shape statistics are used as the atlas or shape prior information.

### 3 Experiments

We validated our method on 36 3D MRI scans. They are from sequences of images over the full cardiac cycle. Thus, the shape variances are large. Manual segmentation was applied in each 2D slice. Then a 3D binary data was obtained by interpolating values among slices. The Marching Cubes method was used to generate a 3D mesh.

These meshes may contain artifacts and too many vertices. Thus geometry processing methods were necessary to downsample and smooth these meshes without removing the shape details. Some decimated meshes are shown in Fig. 3. Fig. 4 visualizes the errors after all geometry processing. The distance between the original surface and the processed surface is computed and visualized. Most errors of vertices are within one voxel. Compared to the initial mesh in Fig. 3, the processed shapes are more smooth and most artifacts are removed, while the shape detail is still preserved. Then, shape

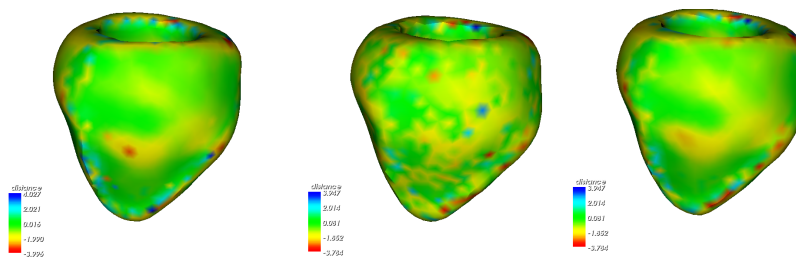


**Fig. 4.** Visual validation of geometry processing methods. The errors of each vertex is plotted using different color. Green means that the error is within one voxel. Blue and yellow denote errors within two voxels.

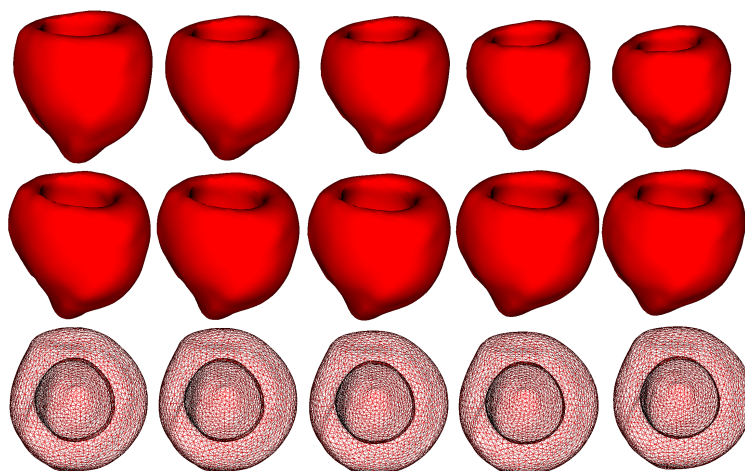


**Fig. 5.** Three modes with largest variations, from  $-3\sigma$  to  $3\sigma$ . The first row: the first mode represents the contraction. The second row: the second mode is the movement along the short axis. The third mode is the twisting.

registration was employed to fit a reference mesh to all the others. This method uses non-rigid local deformation. Thus, the fitted shape is nearly identical to the target shape. Furthermore, the resulting meshes have the same topology and one-to-one correspondence since they all start from the same reference mesh.

After obtaining one-to-one correspondence, it is straightforward to compute the mean shape and its variations, by using generalized Procrustes analysis and PCA. Fig. 5 shows the major modes having largest variances. The first three modes cover more than 80% of the variance. Although the shapes of original data are diverse, the modes are very simple. By changing the variations from  $-3\sigma$  to  $3\sigma$ , where  $\sigma$  is the standard deviation, the first mode just represents the contraction of the heart. The second mode is the movement along the short axis. The third mode is the twisting.

We implemented this method using Python 2.5 and C++ on a Quad CPU 2.4GHZ PC. It took about 20 seconds to do geometry processing and shape registration for each

data, and 5 seconds to construct the atlas and shape statistics from 36 meshes. The processing time may increase when there are more vertices in each shape. In our test, each mesh contained around 2,800 vertices and 5,600 triangles.

## 4 Conclusions

In this paper we presented a framework to construct a 3D shape atlas of the left ventricle from MRI scans. The framework includes geometry processing, shape registration, and Principal Component Analysis. It was tested on 36 annotated 3D data. The benefits of our atlas method are twofold. First, the 3D mesh is generated from existing 2D labeling and MR scans. Thus, 3D training data can be obtained from 2D annotations. Such high-quality meshes can also improve the training performance since points evenly distribute on the surface. Second, the one-to-one correspondences thus established can be used to generate PDM, which is very important for many segmentation methods such as ASM. In the future, we plan to use this atlas to facilitate the segmentation and tracking algorithms, using it as the shape prior information. We will also use this framework to obtain an atlas for other anatomies, such as liver.

## References

1. T. Cootes, C. Taylor, D. Cooper, and J. Graham. Active shape model - their training and application. *CVIU*, 61:38–59, 1995.
2. A. Frangl, D. Rueckert, and J. Duncan. Three-dimensional cardiovascular image analysis. *TMI*, 21(9):1005–1010, 2002.
3. C. Goodall. Procrustes methods in the statistical analysis of shape. *J. Roy. Statistical Society*, 53:285–339, 1991.
4. W. E. Lorensen and H. E. Cline. Marching cubes: A high resolution 3D surface construction algorithm. In *SIGGRAPH*, pages 163–169, 1987.
5. J. Lötjönen, S. Kivistö, J. Koikkalainen, and D. Smutek. Statistical shape model of atria, ventricles and epicardium from short-and long-axis MR images. *Medical image*, Jan 2004.
6. D. Metaxas, L. Axel, Z. Qian, and X. Huang. A segmentation and tracking system for 4D cardiac tagged MR images. *EMBC*, pages 1541–1544, 2008.
7. A. Nealen, T. Igarashi, O. Sorkine, and M. Alexa. Laplacian mesh optimization. In *GRAPHITE*, pages 381–389, 2006.
8. R. Pettigrew and J. Oshinski. MRI techniques for cardiovascular imaging. *Journal Of Magnetic Resoance Imaging*, 10:590 – 601, 1999.
9. D. Shen and C. Davatzikos. An adaptive-focus deformable model using statistical and geometric information. *TPAMI*, 22(8):906 –913, 2000.
10. X. Wang, J. Schaerer, S. Huh, Z. Qian, D. Metaxas, T. Chen, and L. Axel. Reconstruction of detailed left ventricle motion from tMRI using deformable models. *FIMH*, pages 60–69, 2007.
11. H. Zhang, A. Wahle, R. Johnson, T. Scholz, and M. Sonka. 4D cardiac MR image analysis: Left and right ventricular morphology and function. *TMI*, 29(2):350 – 364, 2010.
12. S. Zhang, X. Wang, D. Metaxas, T. Chen, and L. Axel. LV surface reconstruction from sparse tMRI using laplacian surface deformation and optimization. In *ISBI*, pages 698–701, 2009.
13. Y. Zhu, X. Papademetris, A. Sinusas, and J. Duncan. Segmentation of the left ventricle from cardiac MR images using a subject-specific dynamical model. *TMI*, 29(3):669 – 687, 2010.